Sorption of atmospheric gases by bulk lithium metal

C.A. Hart [a], C.H. Skinner [b, *], A.M. Capece [b], B.E. Koel [c]

[a] Department of Physics, University of Maryland, College Park, MD 20742, USA
[b] Princeton Plasma Physics Laboratory, Princeton, NJ 08543, USA
[c] Department of Chemical and Biological Engineering, Princeton University, Princeton, NJ 08544, USA

HIGHLIGHTS

- Li in tokamaks will react with air during maintenance and exposure to residual gases in the vacuum vessel.
- The mass gain of Li samples upon exposure to ambient air indicates conversion to Li_2CO_3.
- Exposure to dry air resulted in a 30 times lower rate of mass gain.
- A rule of thumb for lithium passivation at 26 °C and 45% relative humidity is proposed.

ARTICLE INFO

ABSTRACT

Lithium conditioning of plasma facing components has enhanced the performance of several fusion devices. Elemental lithium will react with air during maintenance activities and with residual gases (H_2O, CO, CO_2) in the vacuum vessel during operations. We have used a mass balance (microgram sensitivity) to measure the mass gain of lithium samples during exposure of a ~1 cm^2 surface to ambient and dry synthetic air. For ambient air, we found an initial mass gain of several mg/h declining to less than 1 mg/h after an hour and decreasing by an order of magnitude after 24 h. A 9 mg sample achieved a final mass gain corresponding to complete conversion to Li_2CO_3 after 5 days. Exposure to dry air resulted in a 30 times lower initial rate of mass gain. The results have implications for the chemical state of lithium plasma facing surfaces and for safe handling of lithium coated components.

© 2015 Elsevier B.V. All rights reserved.

1. Introduction

Lithium conditioning of plasma-facing components has improved plasma performance and reduced recycling on multiple fusion devices [1]. The chemical composition of the lithium surface, which is affected by exposure to ambient air during venting and residual vacuum gases during operation, strongly influences interactions at the plasma−surface interface. Previous studies using X-ray photoelectron spectroscopy (XPS) under ultrahigh vacuum (UHV) conditions have shown that lithium metal films were easily oxidized to a depth of at least 10 nm after exposure to 1−2 Langmuirs (1 L = 1 × 10^{-6} Torr-s) of oxygen or water vapor, corresponding to sticking coefficients of near unity. Exposures to CO_2 or ambient air resulted in an oxidation rate four times smaller than with O_2 or H_2O [2]. The reaction of 7.5-nm lithium films exposed to

O_2 was investigated in a separate study using Auger electron spectroscopy (AES) and ellipsometry and proceeded with an approximately unit reaction probability, though the interpretation of the ellipsometry was complicated by film contraction accompanying the transformation from Li to Li_2O [3]. Oxidation of thicker lithium films exposed to O_2 was investigated by a quartz crystal microbalance and complete conversion to Li_2O occurred within 200 s for films up to 100 nm thick [4]. This work also reported XPS measurements of lithium reactions with water vapor and found the initial formation of one monolayer of oxide followed by the formation of multilayers of hydroxide/oxide mixtures that then converted to oxide over a period of minutes.

In other work, samples of lithium powder with a mass of 0.2 g were exposed to flowing air and its constituent gases at atmospheric pressure and the reactions studied via thermogravimetric analysis (TGA) [5]. In contrast to the thin film results above, no detectable mass gain was observed after exposure to O_2, CO_2, and dry air at temperatures from ambient to 250 °C. However, exposure of lithium to circulating air with 50% relative humidity resulted in

* Corresponding author.
  E-mail address: cskinner@pppl.gov (C.H. Skinner).

mass gain, and the transformation of lithium into lithium compounds was measured over 24 h.

The fundamental theory of the oxidation of thin metallic films was presented in the classic paper by Cabrera and Mott [6]. This theory describes how the oxidation rate depends on film thickness, electric potentials in the film, lattice parameter differences between the metal and metal oxide, and temperature. If the temperature is low enough, metals exposed to oxygen show an initial rapid growth of oxide, followed by a remarkable slowing down once the film thickness reaches some critical thickness of order 10 nm. Xu et al. [7] have presented a model describing the transition from drift-dominated ionic transport for thin films to diffusion-dominated transport for thick films.

Several factors motivate further investigation of the oxidation of thick lithium samples. Thick lithium films are typically used in tokamaks, and measurements of lithium conditioned tiles from the National Spherical Torus Experiment (NSTX) showed that lithium coverage with a 100–500 nm equivalent thickness was required for effective deuterium retention [8]. Future tokamaks may utilize liquid lithium plasma-facing components that take advantage of the benefits of lithium and avoid the limitations due to radiation damage and erosion lifetime of solid materials [9]. In addition, the formation of lithium compounds, such as lithium oxide, as a result of atmospheric gas exposure, has been shown to influence the reactive wettability of liquid lithium [10]. Finally, knowledge of the rate of oxidation or passivation of macroscopic lithium samples is important for the safe handling of lithium and lithium-coated components.

In the present work, lithium samples up to 1-mm thick were exposed to ambient air and dry synthetic air. A microbalance with 1 μg resolution was used to probe mass gain of the samples for time periods of up to two weeks. Optical microscopy monitored changes in surface morphology and color during the exposures and was used to estimate the Pilling–Bedworth [11] ratio (volume change upon oxidation). Section 2 presents the experimental setup, techniques of sample preparation, and analysis of experimental uncertainties. Section 3 reports on the optical microscopy and mass measurements during the exposure to ambient air and interprets the data in terms of the formation of Li_2CO_3. Section 3.2 discusses the results of mass gain after exposure to dry air, and Section 4 summarizes the results.

2. Experimental methods

Lithium sample containers were machined from stainless steel and had an open area of 1 cm^2 and a depth of either 1 mm or 0.3 mm (Fig. 1(A)). The containers were rinsed with water followed by ethanol and then baked at 100 °C to remove adsorbed water before each sample preparation. Lithium rods were obtained from FMC Corporation [12], and were 12-mm in diameter and 165-mm long with a purity of 99.90% by weight (the largest residual impurities levels were up to 150 wppm of Na, Ca, K, N, and Si). The lithium was stored in an argon glove box with oxygen levels reduced to <0.1 ppm and water vapor levels of <1.0 ppm.

Lithium samples were prepared in the argon glove box in three different ways. In the first method, a 1–2 mm slice of lithium was cut from the lithium rod with a stainless steel knife blade in the argon glove box and placed into the well of the stainless steel container. The lithium-filled well was compressed against a stainless steel plate using a C clamp to extrude excess lithium. The sample was then twisted and lifted from the plate and the excess lithium removed from the edges with a knife. This process filled the well and produced a lustrous lithium surface. However, the surface remained rough because some lithium adhered to the stainless steel plate during separation from the lithium well (Fig. 1(B)). The

second method followed the above procedure, but with the lithium surface compressed against a polytetrafluoroethylene (PTFE) plate. Lithium did not adhere well to PTFE, but a weak chemical reaction between lithium and PTFE left a dull surface (Fig. 1(C)). The reaction product was scraped off with a stainless steel plate and a smooth lustrous surface was recovered (Fig. 1(D)). Earlier work found scraping in UHV produced a lithium surface with greater than 95% purity as measured by XPS [2]. In the third method, a small 9 mg sample of lithium was pressed between a pair of stainless steel tabs. The tabs were then separated to obtain lithium samples with a minimal thickness (Fig. 1 (E)). For the dry air exposure experiments, a sample with a smooth surface (Fig. 1(F)) was prepared using the same technique as sample (D). Samples are referenced throughout the text using the lettering assigned in Fig. 1.

The lithium-filled wells were covered with an o-ring sealed enclosure to retain the argon atmosphere during transfer to a separate glove bag for experimental measurements with two mass balances and a digital optical microscope. The lithium-covered stainless steel tab was placed in a sealed plastic container for the same purpose. The primary mass balance, a Sartorius ME-5F, had a precision of 1 μg and was programmed using LabVIEW for automated data logging every 15 s for periods of up to two weeks. The cover of the Sartorius ME-5F weighing chamber remained partially open (1 cm gap) during gas exposures to help maintain the ambient gas composition in light of potential local depletion of individual gas species near the sample. For samples (C–F), automated mass data collection was initiated at least 5 min before exposure of the sample to air. The mass of sample (B) was recorded manually using a Sartorius BB 211S balance with 0.1-mg precision and no weighing chamber. This second balance enabled the study of two samples simultaneously.

The Sartorius ME-5F balance exhibited a small periodic drift under a constant load. Over a 24-h period (12 a.m.–12 p.m.), the rate of drift would oscillate between positive and negative values, with a net positive drift over the course of a day. The drift was correlated with the on/off cycling of the building air conditioning. The average drift rate, 0.01 mg/h, constituted less than 1% of the initial rates of mass gain for the humid air exposures. To correct for this background drift and estimate the associated uncertainty, an empty sample well was measured for five 24-h periods. The drift rates were averaged and fit to a Fourier sine series [Eq. (1)] using a nonlinear least squares method ($r^2 = 0.997$ using 1440 points) to create a continuous drift rate function.

$$f(x) = \sum_{i=1}^{8} a_i * \sin(b_i * t - c_i) \qquad (1)$$

The resultant function used the following coefficients: $a_1 = 0.0479$, $b_1 = 0.240$, $c_1 = 0.306$; $a_2 = 0.0198$, $b_2 = 0.125$, $c_2 = -0.505$; $a_3 = 0.0198$, $b_3 = 0.7873$, $c_3 = 1.75$; $a_4 = 0.0140$, $b_4 = 0.545$, $c_5 = -2.30$, $b_5 = 0.545$, $c_5 = -2.30$; $a_6 = 0.00982$, $b_6 = 1.31$, $c_6 = -2.32$; $a_7 = 0.00760$, $b_7 = 1.57$, $c_7 = 1.03$; $a_8 = 0.00586$, $b_8 = 2.09$, $c_8 = -2.78$. The cumulative background drift was calculated by integrating the drift rate function over the duration of each exposure, and then subtracting this sum from the sample measurements. 1.96 standard deviations of the mean drift rate were used to estimate the uncertainty in the calculated reaction rates (95% confidence interval). Drift functions 1.96 standard deviations above and below the average drift rate were then generated and integrated with respect to time to calculate the background drift's contribution to the uncertainty for each mass measurement. The error bars shown in Figs. 3 and 7 for the rate of mass gain data indicate the uncertainty in calculated values; which is dominated by the uncertainty in the background drift. Figs. 2, 6 and 8 depict the mass gain of samples with error bars corresponding to the integrated uncertainty described above.
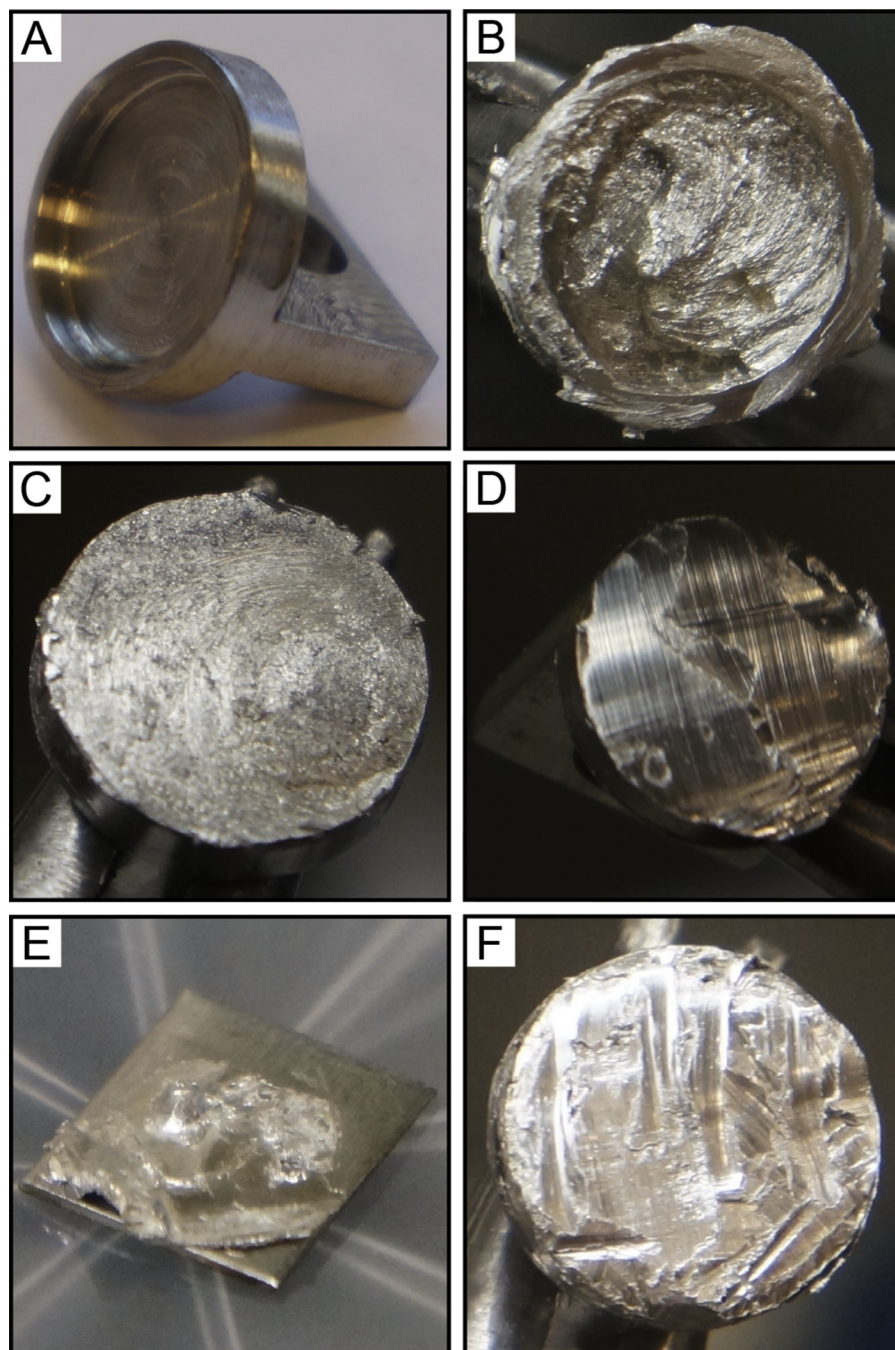
Fig. 1. Samples used in these experiments: (A) empty stainless steel container with 1 mm deep well; (B) lithium sample less than 1 mm thick with a rough surface, after compression against a stainless steel plate and without scraping; (C) lithium sample 1 mm thick with a rough surface after compression onto a PTFE plate and without scraping; (D) lithium sample 0.3 mm thick with a smooth surface after scraping with a stainless steel plate; (E) stainless steel tab with a thin layer of lithium; and (F) 0.3 mm thick lithium sample used for synthetic air experiments. Images were taken in an argon atmosphere before exposure to air.

A National Optical DC3-420T Digital Video Stereo Microscope with a 1.5x magnification objective and 2.0-megapixel camera was used to record images of the lithium surface. The magnification per pixel was estimated by imaging a ruler graduated in tenths of a millimeter and then counting the number of pixels per mm. The image shown in Fig. 5(a) has a magnification of 7.9 ± 0.3 μm per pixel. For the images of sample (E) shown in Fig. 5(b–c) the magnification was 2.5 ± 0.1 μm per pixel.

The temperature and relative humidity inside of the glove bag for experimental measurements were monitored using an Extech

Instruments detector [13], and the values are listed in Table 1. The average measured R.H. during exposures was 45%, which corresponds to a 1.41% atmospheric concentration of water vapor at 25 °C. Comparison of the detector's readings to the weather station at the Princeton Plasma Physics Laboratory demonstrated that temperature and relative humidity measurements for ambient conditions agreed within 1 °C and 2% R.H. after 15 min. For calibration in drier environments, the Extech detector was placed in the argon glove box (<1.0 ppm H_2O). Despite the ultra-low humidity of the argon glove box, the Extech detector continued to
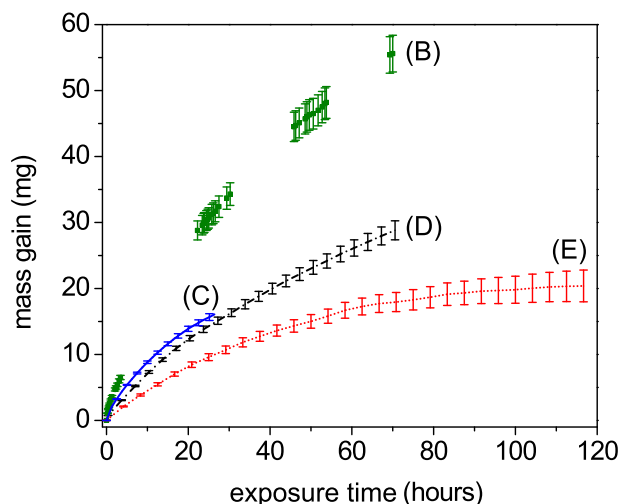
Fig. 2. Mass gain with exposure to ambient air for the samples shown in Fig. 1. Solid curves indicate automated data collected every 15 s. Data points for sample (B) were recorded manually from the BB 211S balance.

measure 18% R.H., (it is not designed to read down to zero). Therefore, we choose to interpret a reading of 18% R.H. on the Extech detector to indicate zero R.H as measured by the glove box meter.

3. Results

3.1. Ambient air exposure

The lithium samples (B–E) shown in Fig. 1 were removed from their transfer enclosures and placed on a balance exposed to ambient air for periods ranging from 1 to 14 days. The mass gain for the first 120 h only is shown in Fig. 2. Sample (D) was transferred to the BB 211S balance and continuous mass gain was measured for 14 days of exposure without saturating. Samples (B) and (C) also did not saturate within their measured exposure times. In contrast, the mass of sample (E) reached a plateau after five days of exposure, increasing by 22.4 mg, from 8.6 to 31 mg, an increase by a factor of 3.6. Calculations based on the density of lithium (0.53 g/cm^3) and Li$_2$CO$_3$ (2.11 g/cm^3), show that complete conversion of the original Li sample to Li$_2$CO$_3$ would result in a final mass of 33.9 mg. The measured final mass of 31 mg agrees with this calculated value within a 95% confidence interval and so after five days sample (E)

was almost all Li$_2$CO$_3$. The exposure time was insufficient to completely convert the larger samples (B–D) to Li$_2$CO$_3$. The mass gain of these samples did not saturate during their exposures (with saturation defined as a mass gain rate within 1.96 standard deviations of the background drift).

Fig. 3(a) shows the rate of mass gain of samples during the first hour of exposure. Fig. 3(b) shows the mass gain over 120 h after smoothing the data after the 7th data point using a centered 15-point (0.06 h) moving average. Table 1 lists the mass gain rate over the first 30 s, 15 min, and 5 h. The estimated balance drift rates for the initial mass gain rates are less than 5% of the values reported in Table 1. These data show a correlation between the rate of mass gain and the roughness and apparent surface area of the sample. Sample (B), which has the roughest surface, exhibits the maximum rate of mass gain. The tab sample (E), which has the smallest apparent surface area, gained mass at the lowest rate, approaching 0.1 mg/h at 60 h. Sample (C), which had a larger apparent surface area than sample (D) initially gained mass at a slower rate, possibly due to contaminants from the reaction between lithium and the PTFE plate during preparation.

The lustrous lithium surfaces imaged in the argon glove box immediately dulled to a dark gray upon exposure to ambient air, as seen in the images of tab sample (E) in Fig. 4. This rapid darkening was attributed to the formation of LiOH in Ref. [5]. Periodically, the samples were transferred from the balance to the microscope for imaging. For the samples (B), (C), (D), and (F), this was done after air exposures of 5 min, 1 h, 5 h, and then daily. For sample tab (E), another similar sample was prepared and was placed under the optical microscope for imaging while the mass of the other sample was measured. Images of tab sample (E) were collected at 5, 15, and 30 min, 1 h, and then hourly intervals for the first 10 h, and daily afterward. Images at select exposure times for sample (E) are shown in Fig. 4 and discussed below to exemplify the optical changes observed in samples (B–E).

After 5 h, the surface developed a translucent film, that appeared white at the edges of the sample and also developed small fractures in the surfaces. After one day of exposure, the surface of the sample appeared less translucent, but not opaque − dark gray coloring remained visible underneath a whitish film. There was no apparent red coloration characteristic of lithium nitride. After three days, the sample appeared white throughout as shown in Fig. 4(d). Although the color did not change after three days, the fractures in the surface continued to grow for the duration of the exposure. Black colored regions on the samples appeared within an hour of exposure to ambient air. These darkly colored regions became more prominent as the sample whitened, appearing
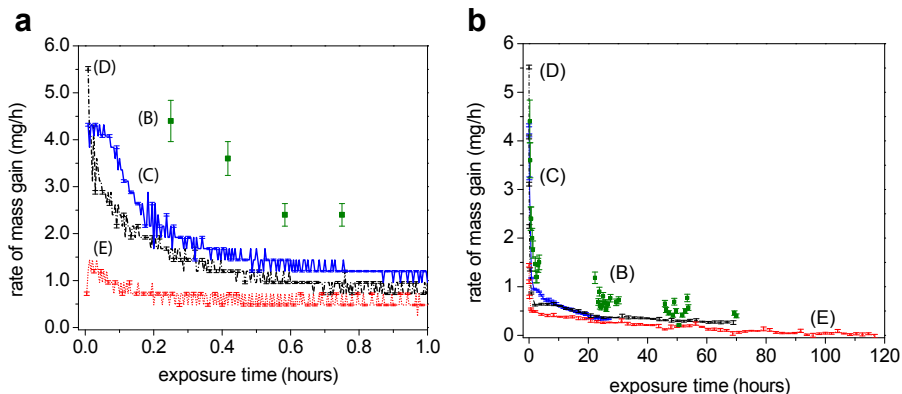

Fig. 3. The rate of mass gain during exposure to ambient air for samples shown in Fig. 1 is shown on a linear scale for (a) the first hour and (b) over 120 h. Data for sample (B) were collected manually from the BB 211S balance and data for samples (C–D) were logged automatically from the ME-5F balance every 15 s.
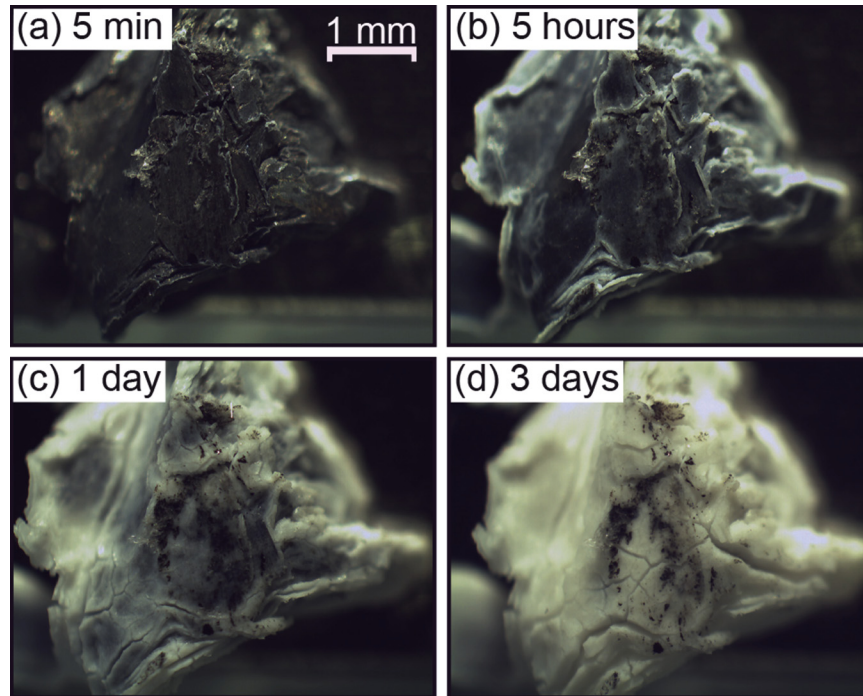
Fig. 4. Changes in appearance of tab sample (E) shown in Fig. 1, during exposure to ambient air as recorded after (a) 5 min, (b) 5 h, (c) 1 day, and (d) 3 days.
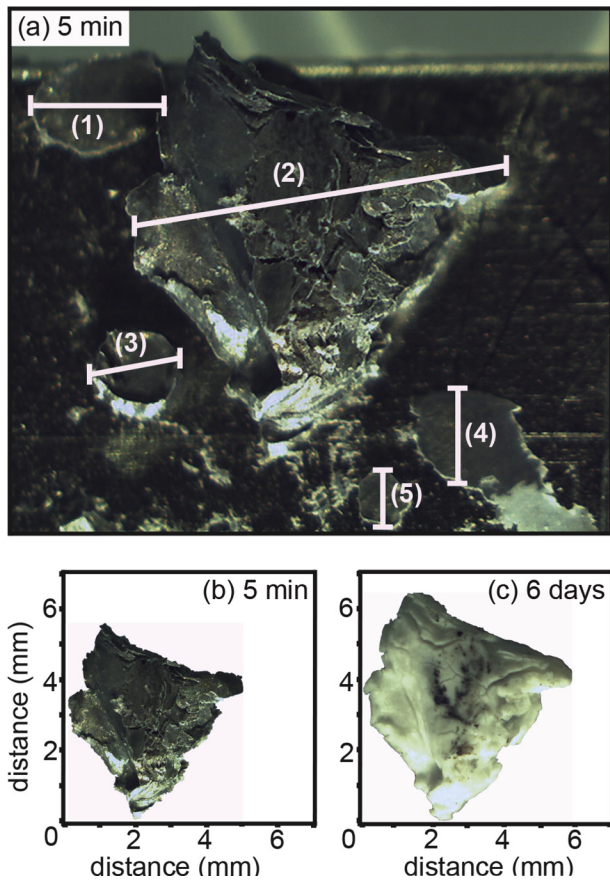
scattered across the surfaces of all samples.

Fig. 5 shows five distinctive features in the images of sample (E). The spatial separations of these features were measured and the percent change in volume was estimated to be 32% by making the approximation of isotropic 3D expansion. In practice the expansion will not be perfectly isotropic as stresses will arise from the progression of the oxidation resulting in surface fractures however this effect is expected to be small. Assuming the final product of lithium exposure to air is Li_2CO_3 [5], a calculation using the density of Li (0.53 g/cm^3) and Li_2CO_3 (2.11 g/cm^3) gives an expected volume

Fig. 5. Optical images of the surface morphology of lithium sample (E) during and after exposure to ambient air. (a) Image after 5 min exposure showing the location of measurements used to calculate volume expansion. Images are shown also for the same sample (b) after 5 min and (c) after 6 days to illustrate the change in volume after exposure to ambient air.
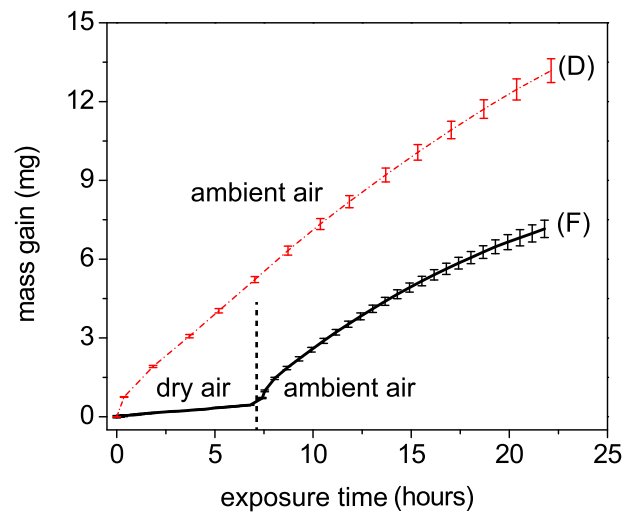
Fig. 6. The influence of water vapor concentration on the oxidation rate of lithium exposed to ambient air. The top, red dashed line is the mass gain of sample (D) in ambient air. This can be compared to the bottom, black line that is the mass gain of sample (F) during an initial exposure to synthetic dry air followed by, after 7 h, additional exposure to ambient air. (For interpretation of the references to color in this figure legend, the reader is referred to the web version of this article.)
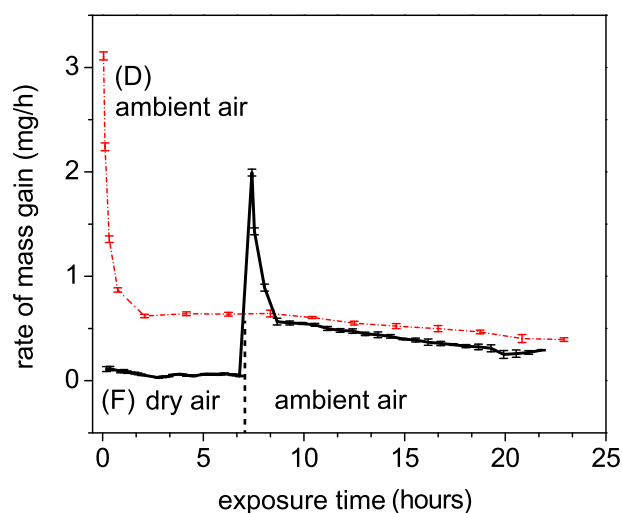
Fig. 7. Influence of reintroducing water vapor on the lithium oxidation rate. The dark, thick line is the rate of mass gain of a lithium sample (F) during initial exposure to synthetic dry air and then after 7 h reintroduction of ambient air containing water vapor. These results can be compared to the red dashed line that is the rate of mass gain of a lithium sample (D) only exposed to ambient air containing water vapor. In synthetic dry air, lithium oxidation proceeds at a rate that is more than ten times slower and nearly constant over the first 7 h. Within 2 h after exposure to ambient air containing water vapor the oxidation rates of the two lithium samples proceed at the same value. (For interpretation of the references to color in this figure legend, the reader is referred to the web version of this article.)
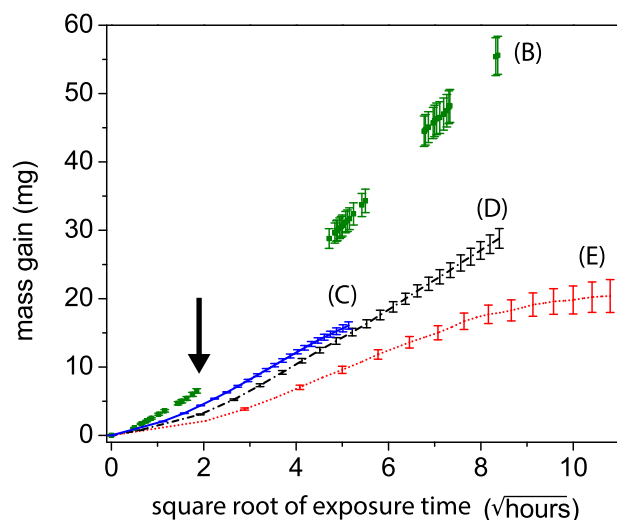

Fig. 8. Plot of the mass gain of lithium samples exposed to ambient air as a function of the square root of the time of exposure. Observation of linear regions in the curves indicates the diffusive nature of the transport causing the mass gain. An inflection point between 4 and 5 h (arrow) correlates with the appearance of fractures on the surfaces of the samples.

increase of 35%. The 32% estimated change in volume approaches this expected value, confirming the almost complete conversion of Li to Li_2CO_3 that was indicated by the mass change reported in Fig. 2. The formation of either LiOH or Li_2O would have resulted in a contraction of these features on the sample.

Pilling and Bedworth [11] concluded in 1923 that metallic oxides with a elementary cell volume exceeding the elementary cell volume of the metal were 'protective' against further oxidation, and conversely, an oxide layer would be 'unprotective' if this ratio was less than unity because the film that forms on the metal surface would be porous and/or cracked. In the present case however, the strain due to the large difference in lattice parameters between Li and Li_2CO_3 produces expansion and fractures in the surface as seen in Fig. 5 (b, c). These fractures expose deeper material and enable continued reactions with air through to complete conversion of the bulk to Li_2CO_3, given sufficient time.

3.2. Dry air exposure

The role of water vapor in the ambient air was isolated by exposing a lithium sample (Fig. 1 F) to synthetic air of composition 78% N_2 and 22% O_2 only. With a dry air flow of 10 l/min through the glove bag, the relative humidity reading decreased from 46% to an apparent 20% R.H. indicated by the Extech meter after 2 h. Prior calibration of this meter in an argon glove box gave a reading of 18% R.H for a <1 ppm H_2O environment, indicating the zero point of the meter. We interpret the R.H. meter reading of 20% as 3.3% R.H., corresponding to 930 ppmv H_2O, by using a linear scaling between 18% and 46%. This value exceeds the manufacturer's specification for the cylinder gas (7 ppm H_2O) and is attributed to the incomplete replacement of the residual ambient air in the glove bag. Nonetheless the synthetic air exposures achieved an order of magnitude reduction in water concentration below the initial >12,000 ppmv for 45% R.H. After 7 h, the flowing synthetic air was terminated, the 310-F mass balance lid fully closed, and the glove bag door opened to reintroduce ambient air. The relative humidity detector reading increased back to 45% R.H and after 15 min, the door was resealed and the lid of the mass balance partially reopened to expose the sample to ambient air. Data collection then continued for another 16 h of exposure to ambient air.

Fig. 6 shows that the rate of mass gain upon exposure to synthetic air was dramatically lower than with ambient air. The initial rate of mass gain of sample (F) was only 0.18 mg/h compared to the rate during exposure to ambient air of 5.5 mg/h for sample (D). This decreased rate of mass gain translated to a similar reduction in accumulated mass gain—only 0.45 mg after 7 h for sample (F) compared to 3.9 mg for sample (D) over the same time period as shown in Fig. 6.

Upon reintroduction of ambient air, the rate of mass gain spiked to 1.99 mg/h as shown in Fig. 7. This rate was significantly greater than that during synthetic air exposure, but less than that for samples initially exposed to ambient air. After the spike, the rate of

Table 1
Rate of mass gain for samples exposed to ambient (B–E) and dry air (F).[a,b]

Sample	Sample mount: Surface quality, thickness	R.H.	Rate of mass gain at 30 s (mg/h)	Rate of mass gain at 15 min (mg/h)	Rate of mass gain at 5 h (mg/h)
B	Well: roughest surface, 1 mm thick	50%	—	4.4 ± 0.8	1.5 ± 0.6
C	Well: rough surface, 1 mm thick	47%	4.32 ± 0.08	2.16 ± 0.04	0.751 ± 0.002
D	Well: smooth surface, 0.3 mm thick	51%	5.52 ± 0.08	1.68 ± 0.06	0.64 ± 0.01
E	Tab: smallest mass, <0.1 mm thick	44%	1.44 ± 0.08	0.73 ± 0.06	0.40 ± 0.01
F	Well: smooth surface, 0.3 mm thick	3.3%[a]	0.18 ± 0.08	0.18 ± 0.08	0.06 ± 0.01

[a] The relative humidity for sample (F) corresponds to an estimated value, not the detector reading, as discussed in Section 4.

[b] The uncertainties reported correspond to values for 1.96 standard deviations.

mass gain then decayed in a manner similar to the other ambient air exposures.

Unlike the ambient air exposures, synthetic air exposures did not result in large observable changes in the lithium samples. After 7 h, the surfaces appeared as lustrous as they were in the argon environment. The surfaces did not turn white, expand, or fracture as they had in ambient air. However, when ambient air was reintroduced such changes began to occur at a similar rate as before. We note that while the ambient air also contains 0.04% CO_2 [14] no reactions between lithium and dry CO_2 up to temperatures of 250 °C were observed in previous studies [5].

4. Discussion

Chemical reactions of lithium with ambient air at 44–51% R.H causes lithium samples to gain mass at high rates initially, which then slowed considerably within a few hours. Initial rates of mass gain up to 5.5 mg/h were observed for one 0.3-mm thick sample (D) with a smooth surface, which had an initial weight of 48 mg. The lithium samples were eventually converted to Li_2CO_3, as evidenced by the mass and volume changes observed. The smallest sample (E), with a mass of 8.6 mg, was completely converted to Li_2CO_3 within 120 h. Experiments with synthetic dry air showed a much lower reaction rate, indicating the primary importance of water vapor in lithium reactions with ambient air. The initial formation of LiOH catalyzes the ultimate conversion of lithium to Li_2CO_3 via the pathway described in Ref. [5]:

$$2Li + 2H_2O \rightarrow 2LiOH + H_2 \tag{2}$$

$$LiOH + CO_2 \rightarrow Li_2CO_3 + H_2O \tag{3}$$

Fissures and cracks open up in the surface from the strain resulting from volume expansion associated with the conversion of lithium to Li_2CO_3, and this also facilitates additional reaction. In order to assess if the film growth follows Wagner's theory of diffusion dominated transport for thick films [7], we plotted the mass gain against the square root of time in Fig. 8 The linearity of this plot indicates a diffusive process, however, there is an inflection between 4 and 5 h of exposure that is correlated with the appearance of surface fractures in optical imagery.

The rate of molecules impinging on a surface calculated from kinetic theory [15] is 2.28×10^{27} m^{-2} s^{-1} at 760 Torr and 26 °C for ambient O_2 and 5.54×10^{25} m^{-2} s^{-1} for ambient H_2O vapor at 45% R.H. in these experiments. From the initial rate of mass gain, measured 30 s after initiating controlled exposure, and using the data for sample (D) given in Table 1 and assuming a surface area twice the geometric value, we calculate a sticking coefficient for O_2 of 5.70×10^{-7} and for H_2O of 2.61×10^{-6}. These values are much lower than the unity sticking coefficients measured under ultrahigh vacuum conditions for both O_2 and H_2O molecules incident on

atomically pure, ultrathin ($\leq$10 nm) films of lithium that were reported previously [2]. Thus, the dynamics of thin film oxidation measured here necessarily takes place on samples that already have thin tarnishing layers on the surface due to the high reactivity of lithium and these films result in much slower oxidation rates for macroscopic samples and coatings.

For safe handling of lithium in NSTX-U that has been exposed to ambient (26 °C, 760 Torr, 45% RH) laboratory air, we have developed a rule of thumb by extrapolating the mass gain shown in Fig. 2 and assuming square-root time dependence until the reaction is complete. Based on this estimate, we suggest the following guideline: a film with 1 μm thickness requires 1 h for passivation, i.e., to fully convert Li to Li_2CO_3 and pose no further reactivity hazards, 10 μm requires one day, and 100 μm (0.1 mm) requires one month. Dry (synthetic) air could be considered as a breathable environment with very reduced lithium reactivity for maintenance activities.

References

[1] M. Ono, et al., Conference report on the 2nd international symposium on lithium applications for fusion devices, Nucl. Fus. 52 (2012) 037001.
[2] C.H. Skinner, R. Sullenberger, B.E. Koel, M.A. Jaworski, H.W. Kugel, J. Nucl. Mater 438 (2013) S647–S650. http://dx.doi.org/10.1016/j.jnucmat.2013.01.136.
[3] K. Wang, P.N. Ross, F. Kong, F. McLarnon, J. Electrochem. Soc. 143 (1996) 422.
[4] K.R. Zavadil, N.R. Armstrong, Surf. Sci. 230 (1990) 47–60.
[5] M.M. Markowitz, D.A. Boryta, J. Chem. Eng. Data 7 (1962) 586.
[6] N. Cabrera, N.F. Mott, Rep. Prog. Phys. 12 (1949) 163.
[7] Z. Xu, K.M. Rosso, S. Bruemmer, Phys. Chem. Chem. Phys. 14 (2012) 14534.
[8] C.N. Taylor, K.E. Luitjohan, B. Heim, L. Kollar, J.P. Allain, C.H. Skinner, H.W. Kugel, R. Kaita, A.L. Roquemore, R. Maingi, Fusion Eng. Des. 88 (2013) 3157. http://dx.doi.org/10.1016/j.fusengdes/2013.09.007.
[9] J.W. Coenen, G. De Temmerman, G. Federici, V. Philipps, G. Sergienko, G. Strohmayer, A. Terra, B. Unterberg, T. Wegener and, D.C.M. Van den Bekerom, Phys. Scr. T. 159 (2014) 01437.
[10] P. Fiflis, A. Press, W. Xu, D. Andruczyk, D. Curreli, D.N. Ruzic, Fusion Eng. Des. 89 (2014) 2827. http://dx.doi.org/10.1016/j.fusengdes.2014.03.060.
[11] N.B. Pilling, R.E. Bedworth, The oxidation of metals at high temperatures, J. Inst. Met. 29 (1923) 529–591.
[12] Seven Lake Pointe Plaza, 2801 Yorkmont Road, Suite 300, Charlotte, NC 2820.
[13] Extech Instruments Corporation, 9 Townsend West, Nashua, NH 03063, U.S.A.
[14] www.esrl.noaa.gov/gmd/ccgg/trends/.
[15] A. Roth, 'Vacuum Technology', third ed., P. 3 Table 1.2 and P. 36.